Mobile Netw Appl (2006) 11:441–449
DOI 10.1007/s11036-006-7192-3

Impulsive noise in UWB systems and its suppression

Youssef Dhibi · Thomas Kaiser

Published online: 4 May 2006

Abstract In this paper we investigate the robustness of mixed impulse radio and UWB-OFDM systems under impulsive noise being typical in UWB multiuser environments. We propose a new receiver structure suppressing iteratively the impulse noise without use of an adaptive clipper. Hence, the delicate problem of tracking a (sub)optimal threshold is avoided. The performance of this structure in comparison with a conventional UWB-OFDM receiver is illustrated.

1. Introduction

Several appealing features, such as high data rates, spectrum reusability, and license-free transmission make UWB systems attractive not only for research but also for future wireless indoor communication systems. In the past decade, a multitude of contributions on UWB have appeared. Beside the impulse radio technology described e.g. in [1, 2], a multi-carrier system based on orthogonal frequency division multiplexing (UWB-OFDM) is also under intensive discussion for a standardized UWB communication system [3, 4].

In contrast to carrier based wireless systems, where different users can be separated by assigning different frequency slots, an UWB system will always be faced with multi-user interference (MUI), which is similar to a CDMA system. This presence of multiple simultaneous users adversely affects the overall performance. The MUI is often considered as an additional additive Gaussian noise component, which is summarized under the key word "Standard Gaussian Assumption," or SGA for short. This assumption has been investigated in detail with special focus on Time-Hopping (TH) Pulse Position Modulation (PPM) based UWB systems. In [5–13], it has been shown that the SGA results in an over-optimistic approximation of the bit error ratio (BER). Recently, the authors have analytically shown [14, 15] the impulsive behavior of the MUI by determining its probability density function (pdf). It was found that the distribution of the MUI is approximated well by the so-called *Middleton class A model (MCA)*, which is often used for modelling impulsive noise [16–18]. The quality of this closed-form approximation was proven by analytic means and further substantiated by simulations. This proven impulsive behavior is described shortly in the first section followed by an introduction of the MCA model.

Taking into further consideration that IR-UWB systems as well as OFDM (Orthogonal Frequency Division Multiplex) based UWB systems will likely coexist in the future commercial mass market, their mutual influence is worth being studied in further detail. Due to the coexistence of both systems, the impulsiveness of the IR-UWB-MUI adversely affects the performance of the conventional UWB-OFDM receiver as shown in Section 4.

Traditionally, impulsive noise suppression in multi-carrier systems are based on signal processing in time domain before demodulation using a clipper [19] and the system performance suffers from it. Another algorithm allowing a satisfactory level of performance is also suggested in [19] suppressing impulsive noise in frequency domain. However, this receiver operates on the complete received vector. Considering the fact that OFDM-reception requires subsets of the receive signal, this structure suppressing impulsive

Y. Dhibi (✉) · T. Kaiser
Department of Communication Systems, Duisburg-Essen University, 47057,Duisburg Germany
e-mail: dhibi@uni-duisburg.de

T. Kaiser
e-mail: thomas.kaiser@uni-duisburg.de

noise is less suitable for UWB-OFDM. Furthermore, this receiver requires a continuous adaption of the threshold value to the noise level.

In this contribution, the major motivation is to avoid the use of a clipper because of a typically *time variant* signal-to-noise ratio (SNR), which requires a continuous adaption of a delicate threshold value. The Sections 5 and 6 describe two new iterative receiver structures suppressing impulsive noise to a large extent. Those receivers are called *UWB-OFDM-IN (UWB-OFDM Receiver for Impulsive Noise)* and *UWB-OFDM-IIN (Iterative UWB-OFDM Receiver for Impulsive Noise)*, respectively. After studying their performance in the case of a deterministic two-path channel, the impact of the IEEE channel model is closer investigated by numerical simulations. A conclusion finishes this contribution.

2. Impulsive behavior of the MUI resulting from IR-UWB systems

Assuming that N_u users transmit their binary data $d^{(u)}(k), u = 1, \ldots, N_u$, simultaneously over N_u time-invariant single-path channels with delays $\tau^{(u)}$, $u = 1, \ldots, N_u$, and attenuations $\alpha^{(u)}, u = 1, \ldots, N_u$, then the received signal $r(t)$ can be written as

$$r(t) = \underbrace{\sum_{l=-\infty}^{+\infty} \sum_{j=lN_s}^{(l+1)N_s-1} \alpha^{(1)} p_T\left(t - \tau^{(1)} - jT_f - c_j^{(1)}T_c - \delta d_l^{(1)}\right)}_{\text{desired signal}}$$
$$+ \underbrace{\sum_{u=2}^{N_u} \sum_{l=-\infty}^{+\infty} \sum_{j=lN_s}^{(l+1)N_s-1} \alpha^{(u)} p_T\left(t - \tau^{(u)} - jT_f - c_j^{(u)}T_c - \delta d_l^{(u)}\right)}_{\text{multiuser interference } n_{\mathrm{MUI}}(t)}$$
$$+ n_\mathrm{G}(t), \tag{1}$$

where $p_\mathrm{T}(t)$ represents the transmitted pulse shape and is often modelled according to [20] as the normalized second Gaussian derivative

$$p_T(t) = K_p \left[1 - 4\pi \left(\frac{t}{\tau_p}\right)^2\right] \exp\left(-2\pi \left(\frac{t}{\tau_p}\right)^2\right). \tag{2}$$

K_p is a normalization factor yielding a unit-energy pulse. N_s is the number of pulses used to transmit a single information bit, T_f is the duration of one frame. The bit duration is $T_b = N_s T_f$, T_c is the chip duration, $\mathrm{c}_j^{(u)}$ represents the random TH code of the u-th user, δ describes the time shift associated with the PPM, and τ_p is the time normalization factor determining the width of the transmit pulse. All parameters are described in detail in [1, 2].

The value of the output variable Z of an over-all correlator at the receiver side used by the TH-PPM-UWB system depends on the position of the interfering signal. By studying its behavior, an analytical expression of the MUI-pdf is given by [14, 15]

$$f_X^{\mathrm{MUI}}(x) = \sum_{\mu=0}^{n} \frac{A^\mu \mathrm{e}^{-A}}{\mu! \sqrt{2\pi\sigma_\mu^2}} \mathrm{e}^{-\frac{x^2}{2\sigma_\mu^2}}, \tag{3}$$

which describes the mentioned MCA noise model [16–18]. A is the so-called *impulsiveness parameter*, and it depends on all system parameters given above (see [14, 15] for the exact relation and the detailed discussion of all parameters).

For a better understanding of the exact behavior of the MUI, a short description of the MCA model is given in the following.

3. Middleton class a noise

3.1. Definitions and properties

The MCA model [16–18] has been found to provide good fits to a variety of noise and interference measurements [16, 21]. Actually, the MCA noise model is used to describe *narrowband* noise as its *envelope*.

The pdf $f_{\mathrm{MCA}}(x)$ of this noise model is defined as an "infinite weighted sum of Gaussian densities with decreasing weights for Gaussian densities with increasing variances." $f_{\mathrm{MCA}}(x)$ is given by (4) containing a Gaussian component and an independent additive interference component originating from a Poisson mechanism

$$f_{\mathrm{MCA}}(x) = \sum_{m=0}^{\infty} \frac{\mathrm{e}^{-A} A^m}{m!} \frac{1}{\sqrt{2\pi\sigma_m^2}} \mathrm{e}^{-\frac{x^2}{2\sigma_m^2}}. \tag{4}$$

The major appeal of this model is that its parameters can be directly physically interpreted. The parameter A is called the *impulsive index* and describes the *impulsiveness* of the noise. A small value of A implies a highly impulsive interference (see Fig. 1). The variances σ_m^2 are functions of the parameter γ_A, defined as the ratio of the power in the Gaussian noise component (σ_G^2) to the power of the interfering Poisson process (σ_P^2) [22]

$$\sigma_m^2 = \frac{\frac{m}{A} + \gamma_A}{1 + \gamma_A} \quad \text{with} \quad \gamma_A = \frac{\sigma_G^2}{\sigma_P^2}. \tag{5}$$

The pdf is illustrated in Fig. 1 for different values of A. In Fig. 2, the impact of γ_A is illustrated.

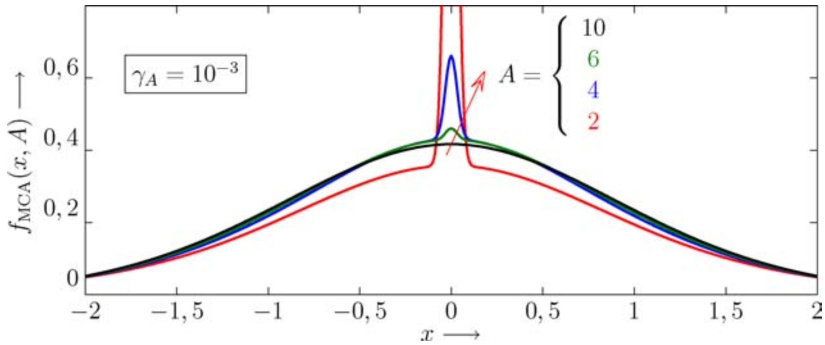

Fig. 1 Middleton Class A model (A variable, $\gamma_A = 10^{-3}$)

The impact of the parameter A on the behavior of the pdf can be summarized as follows:

- For large A, the variance σ_m^2 does not depend on m. According to Eq. (5) we get

$$\lim_{A\to\infty} \sigma_m^2 = \lim_{A\to\infty} \frac{\frac{m}{A} + \gamma_A}{1+\gamma_A} = \frac{\gamma_A}{1+\gamma_A} \neq f(m).$$

Consequently, the pdf $f_{\mathrm{MCA}}(x)$ approaches the Gaussian density presenting the limiting case of the MCA model and Eq. (4) reduces to

$$\begin{aligned}\lim_{A\to\infty} f_{\mathrm{MCA}}(x) &= \lim_{A\to\infty} \sum_{m=0}^{\infty} \frac{\mathrm{e}^{-A}A^m}{m!} \frac{\mathrm{e}^{-\frac{x^2}{2\sigma_m^2}}}{\sqrt{2\pi\sigma_m^2}} \\ &= \lim_{A\to\infty} \frac{\mathrm{e}^{-A}}{\sqrt{2\pi\frac{\gamma_A}{1+\gamma_A}}} \mathrm{e}^{-\frac{x^2}{2\frac{\gamma_A}{1+\gamma_A}}} \underbrace{\sum_{m=0}^{\infty}\frac{A^m}{m!}}_{=\mathrm{e}^A} \\ &= \lim_{A\to\infty} \underbrace{\mathrm{e}^A\mathrm{e}^{-A}}_{=1} \frac{1}{\sqrt{\frac{2\pi\gamma_A}{1+\gamma_A}}} \mathrm{e}^{-\frac{x^2}{\frac{2\gamma_A}{1+\gamma_A}}} \\ &= \frac{1}{\sqrt{\frac{2\pi\gamma_A}{1+\gamma_A}}} \mathrm{e}^{-\frac{x^2}{\frac{2\gamma_A}{1+\gamma_A}}}.\end{aligned}$$

- For small A, the MCA pdf becomes more impulsive due to larger "tails". Hence, only a small number of terms in Eq. (4) remains, since the factor $p_m = \frac{A^m}{m!}$ tends to zero for small A and $m \geq 3$. It can be shown [23] that the pdf can be approximated by piecewise defined function

$$f_{\mathrm{sMCA}}(x, A) = \max_{m=0,1,2} \left[\frac{\mathrm{e}^{-A}A^m}{m!\sqrt{2\pi\sigma_m^2}} \mathrm{e}^{-\frac{x^2}{2\sigma_m^2}} \right], \tag{6}$$

where the notation "sMCA" stands for *simplified* MCA model. It follows [23, 24]

$$f_{\mathrm{sMCA}}(x, A) = \begin{cases} \frac{\mathrm{e}^{-A}}{\sqrt{2\pi\sigma_0^2}}\mathrm{e}^{-\frac{x^2}{2\sigma_0^2}} & \text{for } 0 \leq |x| < a = \sqrt{\frac{2\sigma_0^2\sigma_1^2}{\sigma_0^2-\sigma_1^2}\ln\left(\frac{\sigma_0}{\sigma_1}A\right)} \\ \frac{\mathrm{e}^{-A}A}{\sqrt{2\pi\sigma_1^2}}\mathrm{e}^{-\frac{x^2}{2\sigma_1^2}} & \text{for } a \leq |x| < b = \sqrt{\frac{2\sigma_1^2\sigma_2^2}{\sigma_1^2-\sigma_2^2}\ln\left(\frac{\sigma_1}{2\sigma_2}A\right)} \\ \frac{\mathrm{e}^{-A}A^2}{2\sqrt{4\pi\sigma_2^2}}\mathrm{e}^{-\frac{x^2}{2\sigma_2^2}} & \text{for } b \leq |x| \end{cases}$$

with the variances $\sigma_0^2 = \frac{\gamma_A}{1+\gamma_A}$, $\sigma_1^2 = \frac{1/A+\gamma_A}{1+\gamma_A}$ and $\sigma_2^2 = \frac{2/A+\gamma_A}{1+\gamma_A}$.

The quality of approximation for small A is confirmed by the curves shown in Fig. 3.

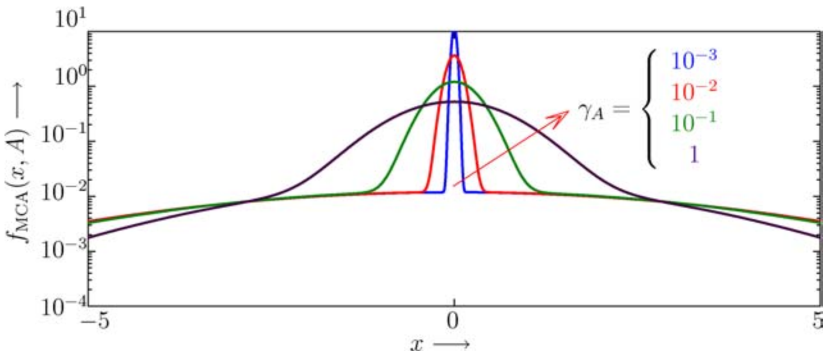

Fig. 2 Middleton Class A model (γ_A variable, $A = 10^{-1}$)

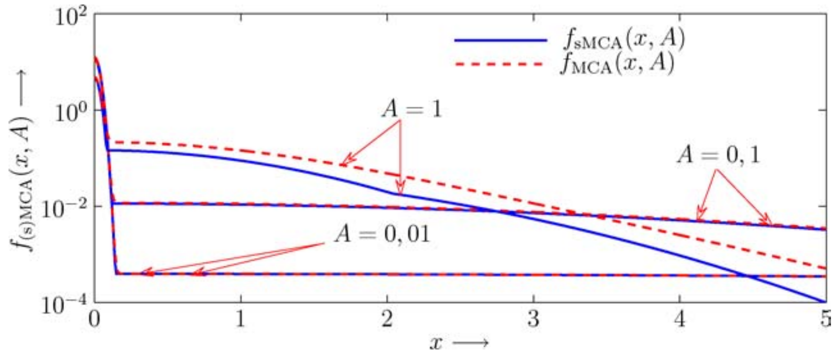

Fig. 3 Simplified pdf of the MCA model ($\gamma_A = 10^{-3}$)

3.2. Noise consideration

In the following we neglect for simplicity the thermal noise mainly because the MCA model already contains a Gaussian noise component as mentioned above. Moreover, both discussed receiver structures can be compared by signal-to-interference ratio (SIR) on behalf of signal to interference plus noise ratio only. Note that the definition of E_b/N_0 remains the same as in case of pure additive Gaussian noise, since the variance of the MCA is finite.[1]

4. Impact of additive impulsive noise

4.1. General consideration

The impact of impulsive noise can be studied by comparing the performance of an AWGN- with that one of an *AWIN-channel (additive white impulsive noise)* in terms of the BER. In the first case we get

$$\text{BER}_{\text{AWGN}} = \frac{1}{2}\text{erfc}\left(\sqrt{\frac{E_b}{N_0}}\right).$$

Considering an AWIN-channel with additive impulsive noise described by the MCA model we obtain [14]

$$\text{BER}_{\text{AWIN}} = \frac{1}{2}\sum_{m=0}^{+\infty}\frac{\mathrm{e}^{-A}A^m}{m!}\text{erfc}\left(\sqrt{\frac{A\gamma_A + A}{A\gamma_A + m}\frac{E_b}{N_0}}\right).$$

The parameters used here are as defined in the previous section. The behavior of both equations. is illustrated in Fig. 4 for different impulsiveness parameters.

According to the impulsiveness of the additive noise, the BER_{AWIN} is already for small SNR values lower than BER_{AWGN}. Furthermore, it has a lower decay for higher SNR values. This behavior results directly from the properties of

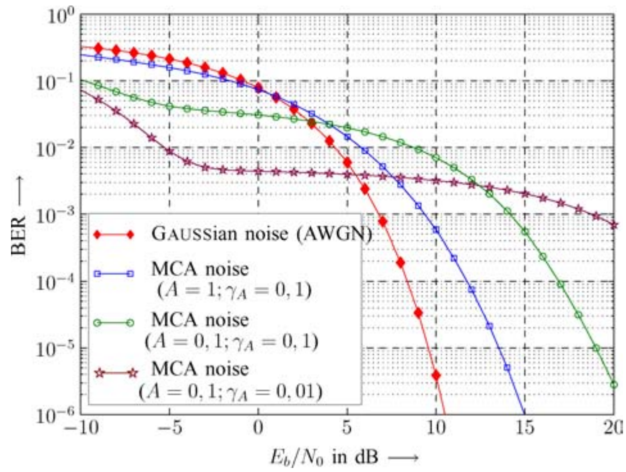

Fig. 4 BER in case of an AWGN- and an AWIN-channel

impulsive noise which is characterized by a certain number of "impulses" with higher amplitudes. This number depends directly from the impulsiveness of the noise: the higher this impulsiveness, the higher are the amplitudes of the impulses and the smaller is their number. Therefore, more transmit power is required in order to get a lower BER.

Due to reflections, scattering, and dispersion effects in real-world environments, the channels are not well described by a pure AWGN- or AWIN-model. Hence, for more reliable results the multipath propagation has to be taken adequately into account. This is done in the following section by considering a conventional UWB-OFDM system.

4.2. Conventional UWB-OFDM system

In order to study the robustness of a UWB-OFDM receiver against impulsive noise we briefly revisit the conventional receiver first. Further details are given in [25].

The transceiver structure is illustrated in Fig. 5. Note that for sake of simplicity, the QPSK modulation scheme used in this system is not shown explicitly. According to one of the major proposal for standardization [25], a 128 points FFT (IFFT) is deployed in the receiver (transmitter), respectively.

[1] Some impulsive noise models show infinite variance, then the definition of an SIR etc. becomes rather delicate.

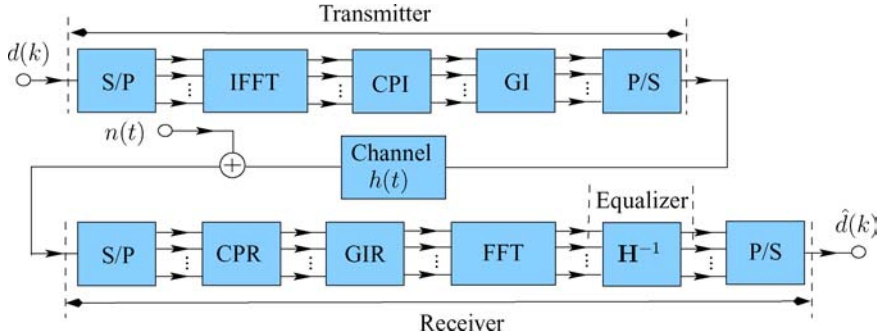

Fig. 5 Conventional UWB-OFDM transceiver; CPI: Cyclic Prefix Insertion, GI: Guard Interval, P/S: Parallel-to-Serial, S/P: Serial-to-Parallel, CPR: Cyclic Prefix Removal, GIR: Guard Interval Removal

The further parameters of an uncoded UWB-OFDM system are summarized in Table 1. The robustness of UWB-OFDM in presence of impulsive noise can be numerically investigated by adequate modelling of the additive noise, i.e. by the MCA model. A deterministic two-path channel with the path loss coefficients $\alpha_0 = 1$ and $\alpha_1 = j0.5$ is applied in the following (see also the discussion in Section 5). The performance of the conventional receiver is shown in Fig. 6 for different types of noise: the BER decreases with increasing impulsiveness of the noise, which is in good agreement with the definition of the MCA distribution tending to be GAUSSIAN for larger

In order to suppress impulsive noise, a clipper is often used in communication systems. However, as mentioned earlier, tracking of the threshold is a rather delicate task. Thus, it is recommended to develop receiver architectures that do not employ a clipper but allow alternative impulsive noise suppression schemes. In the following, we propose a "clipper-free" *UWB-OFDM receiver for Impulsive Noise* (UWB-OFDM-IN).

5. UWB-OFDM-IN

5.1. Description

The proposed UWB-OFDM-IN is depicted in Fig. 7. Note that although our new receiver requires blockwise processing, we will use a scalar notation for reasons of simplicity.

Table 1 Parameters of an uncoded UWB-OFDM system

Bandwidth	528 MHz
Number of Total Subcarriers	128
Number of Data subcarriers	100
Information Duration	242,4 ns
Length of the CP	60,6 ns
Length of the GI	9,5 ns
Symbol Duration	312,5 ns (242, 4s + 60, 6s + 9, 5s)
Modulation	QPSK
Bitrate	640 Mb/s

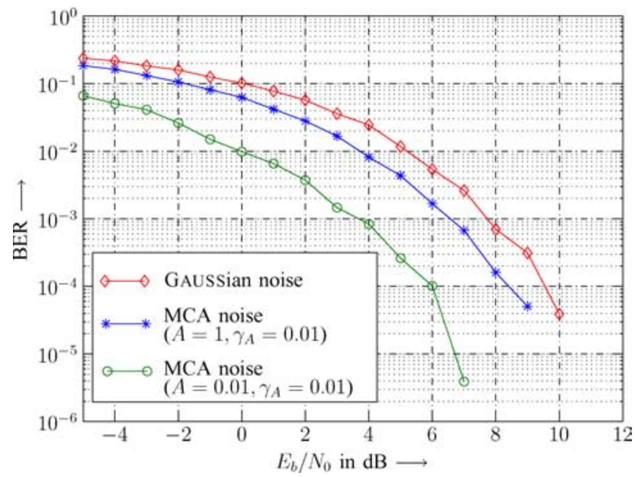

Fig. 6 Performance of a conventional UWB-OFDM receiver in an impulsive environment

The blockwise processing causes some inherent delay and can be realized by a suitable designed memory but does not mean any loss of generality. Our approach works as follows.

Let $d(n) \in [\pm 1, \pm j]$, $n = 0, \ldots, N-1$ be the QPSK-modulated complex user data. The output of the conventional OFDM modulator (Fig. 5, after IFFT), denoted as $s(k)$, is given by

$$s(k) = \frac{1}{N} \sum_{n=0}^{N-1} d(n)\, \mathrm{e}^{j2\pi nk/N}. \tag{8}$$

The received signal[2] $r(k) = h(k) * s(k) + n(k)$ is demodulated by a conventional UWB-OFDM demodulator (Fig. 5). The output of this receiver is denoted by $\hat{d}(n), n = 0, \ldots, N-1$.

In order to combat the impulsiveness without use of a clipper, the conventional structure is extended by the following processing steps: The (demodulated) data $\hat{d}(k)$ is *re*modulated by an OFDM modulator (Fig. 7). The resulting signal $h(k) * \hat{s}(k)$ is then subtracted from the original

[2] CPI, GI, ... , are omitted here to keep the notation simple.

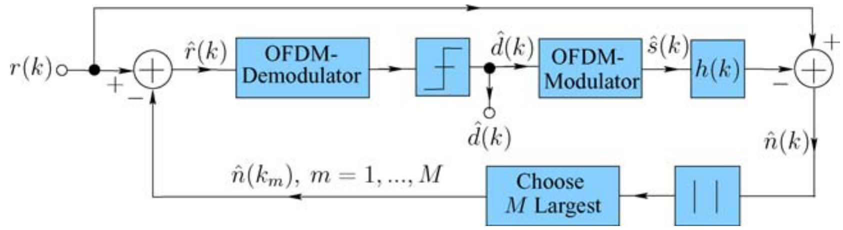

Fig. 7 UWB-OFDM receiver for impulsive noise

received data synchronously. In such a way, we obtain a noise estimate $\hat{n}(k) = r(k) - h(k) * \hat{s}(k)$. The largest M values are then fed back to the input of the demodulator, subtracted synchronously from the received signal, and then demodulated again. The choice of M is investigated later. This subtraction allows the partial replacement of the high noise amplitudes by lower ones yielding the desired noise suppression.

The following investigations are carried out for two cases: For sake of simplicity we start with a simple deterministic two-path transmission channel and the path loss coefficients $\alpha_0 = 1$ and $\alpha_1 = j0.5$. Then, we extend the study to a dense multipath environment [26], which is typical for UWB transmission.

Let us briefly discuss how to mathematically handle the number M of fed back values. If the M largest values are fed back into the demodulator, the signal samples

$$r(k_m) - \hat{n}(k_m) = \hat{r}(k_m), \quad m = 1, \ldots, M,$$

are obtained. Thus, the M large noise amplitudes are replaced by lower ones, which realizes the suppression process. The modified received signal can be written as

$$\hat{r}(k) = \begin{cases} \hat{r}(k_m) & \text{for } m = 1, \ldots, M \\ r(k) & \text{for } \quad k \neq k_m. \end{cases}$$

5.2. Simulations

The performance of the UWB-OFDM-IN receiver is evaluated by a comparison with a conventional UWB-OFDM receiver. The impulsive noise is generated by the MCA model with the parameters $A = 0.01$ and $\gamma_A = 0.01$ and M is set to $M = 10$. The corresponding simulation results are given in Fig. 8, where also the performance of the conventional UWB-OFDM receiver in a Gaussian environment is shown. As it can be seen, the proposed receiver outperforms the conventional one with a gain of more than 3 dB at a BER of 10^{-3}.

Due to the involved nonlinearities and iterations, the proposed receiver structure can not be mathematically handled in closed form. Hence, we have to investigate the impact of M by simulations only. Observe first, that the higher the impulsiveness, the larger M. Second, in order to gain more insight, the BER is evaluated for different values of the signal-to-noise ratio as a function of M. In such a way the optimal M can be found. The result of this experiment is given in Fig. 9, where the noise remains unchanged.

It can be observed that the optimal M for the chosen channel lies in the range between 10 and 13. This constant interval is due to the fact that the parameters of the noise are kept unchanged. The independency of M on E_b/N_0 is explained by the fixed parameters of the impulsive

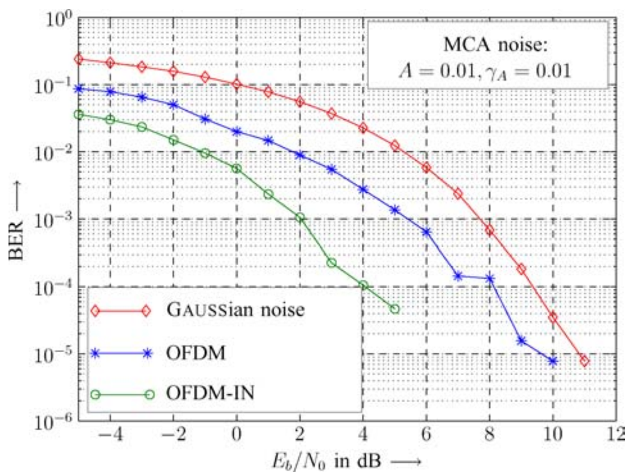

Fig. 8 Performance of UWB-OFDM-IN in comparison with a conventional receiver ($M = 10$)

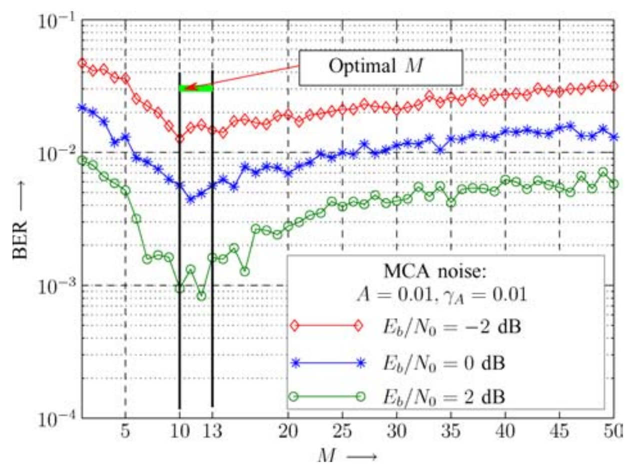

Fig. 9 BER as a function of M

noise implying a constant ratio γ_A between the Gaussian background noise and the impulsive component as described by the MCA model (see Section 2).

In order to determine this range for different noise parameters, the experiment has to be repeated. Further simulations have shown that the optimal range of M is shifted to higher values with increasing the impulsiveness. This means that the number M has to be determined in an adaptive way for a time-variant multiuser scenario and is therefore—similiar to the time variant SNR threshold—difficult to analyze and to track. Hence, we propose a further approach. The basic idea is to choose M relatively small and keep it fixed in order to minimize the numerical effort. To achieve the desired suppression, the UWB-OFDM-IN is repeated iteratively. Doing this, we obtain a new receiver with the same basic structure, so we call it *Iterative UWB-OFDM receiver for impulsive noise* (UWB-OFDM-IIN) and is closer investigated in the following.

6. UWB-OFDM-IIN

In order to demonstrate the improvement of this iterative structure, the previous experiment is repeated. The results are shown in Fig. 10 confirming that the UWB-OFDM-IIN receiver outperforms all other structures: In a case of small $M = 5$ and only 3 iterations we note an additional gain of approximately 2 dB in comparison to UWB-OFDM-IN. This results in a total gain of approximately 8 dB compared to the conventional UWB-OFDM receiver under Gaussian noise environments as discussed in the UWB-OFDM proposal for standardization.

The previous results were obtained in case of a simple deterministic two-path channel. For a realistic UWB environment, the standardized channel model [26] characterizes

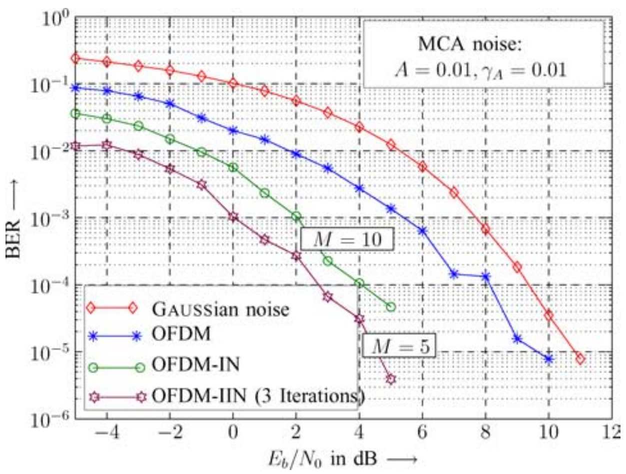

Fig. 10 Performance of the proposed iterative receiver compared with the non-iterative and conventional UWB-OFDM receiver

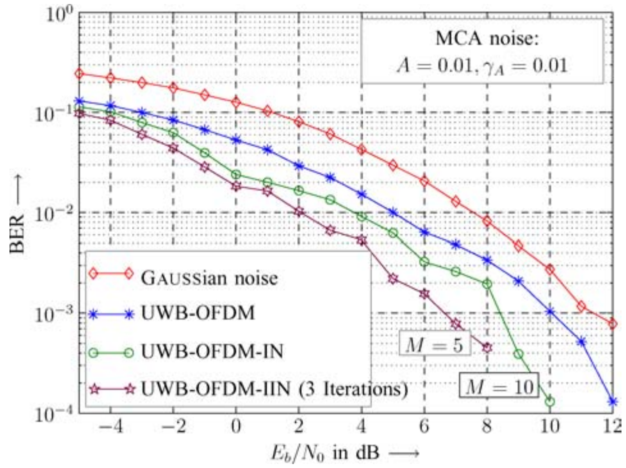

Fig. 11 Performance of the UWB-OFDM-IN and UWB-OFDM-IIN receivers in comparison with a conventional UWB-OFDM receiver under impulsive noise in a typical dense multipath UWB environment (channel Model CM1)

the dense multipath adequately and is therefore taken into account. Its impulse response $h(t)$ is based on the so-called Saleh-Valenzuela model (SV model) [27] and is composed by L clusters containing K rays each [26, 28, 29]

$$h(t) = \sum_{l=1}^{L} \sum_{k=1}^{K} \alpha_{k,l}\delta(t - T_l - \tau_{k,l}). \tag{9}$$

The constants $\alpha_{k,l}$ and $\tau_{k,l}$ are the path loss and channel delay coefficients, respectively. Note that 4 models– CM1, CM2, CM3 and CM4—are introduced representing different environments. For example, a dense multipath environment with line of sight (LOS) is characterized by CM1 while CM2 describes the same without LOS (non-line of sight, NLOS).

In this contribution, we show the simulation results obtained for the CM1 channel model. In case of other environments the same principle behavior was noticed. Furthermore, we assume that the channel coefficients needed for the equalization (see Fig. 5) are known at the receiver. This can be achieved by conventional algorithms for channel estimation [30].

Figure 11 shows the performance of the proposed receivers in comparison with the conventional one, where the noise follows again the MCA model. The results confirm a slightly lower total gain of approximately 5 dB in comparison with the conventional UWB-OFDM receiver in a Gaussian environment. In case of impulsive noise, a gain of approximately 3 dB can be achieved.

7. Conclusion

In this contribution, the conventional UWB-OFDM receiver structure has been extended by taking into account the impulsiveness of impulse radio based multiuser interferences. In conventional receiver structures, a clipper is usually deployed for combating impulsive distortions. Its threshold value has to be continuously adapted to the time variant noise level, which turns out to be rather delicate in practical scenarios. Here, we propose alternative "clipper-free" UWB-OFDM receivers. A gain of approximately 6 dB is observed for an unrealistic two-path channel and approximately of 3 dB even in a dense multipath environment. Future work will cover the impact of interleaving and coding, where the latter is not only of relevance for OFDM but especially for iterative noise suppression schemes.

References

1. M.Z. Win and R.A. Scholtz, Impulse Radio: How It Works, IEEE Communication Letters 2(2) (Februar 1998) 10–12.
2. M.Z. Win and R.A. Scholtz, Ultra-wide bandwidth time-hopping spread-spectrum impulse radio for wireless multiple-access communications, IEEE Transactions on Communications 48(4) (April 2000) 679–691.
3. A. Batra, IEEE P802.15 Working Group for Wireless Personal Area Networks (WPANs), September 2003.
4. A. Batra and et al., IEEE P802.15 Wireless Personal Area Networks, November 2003.
5. B. Hu and N. Beaulieu, Exact bit error rate analysis of TH-PPM UWB systems in the presence of multiple-access interference, IEEE Communications Letters 7(12) (Dec!ember 2003) 572–574.
6. G. Durisi and S. Benedetto, Performance evaluation of TH-PPM UWB systems in the presence of multiuser interference, IEEE Communications Letters 7(5) (May 2003) 224–226.
7. G. Durisi and S. Benedetto, Performance evaluation and comparison of different modulation schemes for UWB multiaccess systems, ICC, Anchorage, USA, pp. 2187–2191, 11–15 May 2003.
8. G. Durisi and G. Romano, Simulation analysis and performance evaluation of an UWB system in indoor multipath channel, in IEEE Conference on Ultra Wideband Systems and Technologies, Digest of Papers, Baltimore, USA, 157–161, 2002, pp 2002.
9. G. Durisi, J. Romme and S. Benedetto, Performance of TH and DS UWB multiaccess systems in presence of multipath channel and narrowband interference, (IWUWBS, Oulu, Finnland, November 2003).
10. G. Durisi and G. Romano, On the validity of gaussian approximation to characterize the multiuser capacity of UWB TH PPM, in: Proc. IEEE Conf. on Ultra Wideband Systems and Technologies 2002, Digest of Papers (2002), pp. 157–162.
11. J. Fiorina and W. Hachem, Central limit results for the multiple user interference at the SUMF output for UWB signals, (SITA 2004 ,Parama, Italien, 2004).
12. M. Sabattini, E. Masry and L.B. Milstein, A Non-gaussian approach to the performance analysis of UWB TH-BPPM systems, in IEEE Conference on Ultra Wideband Systems and Technologies, , (16–19 November 2003). pp. 52– 55.
13. M.-G. DiBenedetto and G. Giancola, *Understanding Ultra Wide Band Radio Fundamentals*, 1st ed., ser. Prentice Hall Communications Engineering and Emerging Technologies Series. Prentice Hall PTR, Juni (2004).
14. Y. Dhibi, Impulsive Kanalstrungen und deren Einfluss in Ultrabreitbandigen übertragung (Impulsive Noise and its Impact in UWB Systems), Ph.D. dissertation, Universität Duisburg-Essen, July 2005.
15. Y. Dhibi and T. Kaiser, On the Impulsiveness of Multiuser Interferences in TH-PPM-UWB-Systems, To appear in IEEE Transactions on Signal Processing, (2005).
16. D. Middleton, Statistical Models of Electromagnetic Interference, IEEE Transactions on Electromagnetic Compatibility EMC-19(3) (August 1977) 106–127.
17. A. D. Spaulding and D. Middleton, Optimum Reception in an Impulsive Interference Environment–Part I: Coherent Detection, IEEE Transactions on Communications COM-25(9) (September 1977) 910–923.
18. D. Middleton, Procedures for determing the parameter of the first-order canonical models of class A and class B electromagnetic interference, IEEE Transactions on Electrometromagnetic Compatibility EMC-21 (1979) 209–220.
19. S.V. Zhidkov, Impulsive noise suppression in OFDM-based communication systems, IEEE Transactions on Consumer Electronics 49(3) (November 2003) 944–948.
20. R.A. Scholtz, Multiple access with time-hopping impulse modulation, IEEE Military Communications Conference 2 (October 1993) 447–450.
21. S.A. Kassam, *Signal Detection in Non-Gaussian Noise* (Berlin: Springer-Verlag, 1988).
22. S. Unawong, S. Miyamoto and N. Morinaga, A novel receiver design for DS-CDMA systems under impulsive radio noise environments, IEICE Transactions on Communications E82-B(6) (June 1999).
23. Y. Nakano, D. Umehara, M. Kawai and Y. Morihiro, Viterbi decoding for convolutional code over Class A noise channel, in: *Proceedings of the 7th International Symposium on Power-Line Communications and Its Applications, Kyoto, Japan,* (2003) pp. 97–102.
24. L.A. Berry, Understanding middleton's canonical formula for class a noise, IEEE Trans Electromagn Compat EMC-23(4) (November 1981) 337–344.
25. A. Batra and et al., TI physical layer proposal, Project: IEEE P802.15 Working Group for Wireless Personal Area Networks (WPANs), (May 2003).
26. A.F. Molisch, J.R. Foerster and M. Pendergrass, Channel models for ultrawideband personal area networks, IEEE Personal Communications Magazine 10 (December 2003) 14–21.
27. A. Saleh and R. Valenzuela, A statistical model for indoor multipath propagation, IEEE JSAC SAC-5(2) (February 1987) 128–137.
28. D. Cassioli, M.Z. Win and A.F. Molisch, The ultra-wide bandwidth indoor channel: From statistical model to simulations, IEEE Journal on Selected Areas in Communications 20(6) (August 2002) 1247–1257.
29. J.R. Foerster, M. Pendergrass and A.F. Molisch, A channel model for ultrawideband indoor communication, Technical Report of MERL TR-2003-73 (November 2003).
30. V. Lottici, A. D'Andrea and U. Mengali, Channel estimation for ultra-wideband communications, IEEE Journal on Selected Areas in Communications 20(9) (December 2002) 1638–1645.

Youssef Dhibi has studied electrical engineering from 1995 to 2000 at the Duisburg-Essen University and received there his diploma on September 2000. The title of the diploma thesis was "Taktsynchronisierung mit Statistiken höherer Ordnung" (Synchronisation with Higher Order Statistics). Since September 2000 to July 2005 he worked as research assistant (PhD student) in the Department of Communication Systems at the university Duisburg-Essen where he got his PhD in July 2005. The title of the PhD-thesis was "Impulsive Kanalstörungen und deren Einfluss in der Ultrabreitbandigen Übertragung" (Impulsive Noise and its Impact in Ultrawide Band Communications). He is now still in the Department of Communication Systems at the university Duisburg-Essen as research assistant. His research domains are Impulsive Noise and Signal processing for Ultrawide Band Systems.

Thomas Kaiser (SM'04) received the Ph.D. degree in 1995 with distinction and the German habilitation degree in 2000, both from Gerhard-Mercator-University Duisburg and in electrical engineering. From April 2000 to March 2001 he was the head of the Department of Communication Systems at Gerhard-Mercator-University Duisburg and from April 2001 to March 2002 he was the head of the Department of Wireless Chips & Systems (WCS) at Fraunhofer Institute of Microelectronic Circuits and Systems. In summer 2005 he joined Stanford's Smart Antenna Research Group (SARG) as a visiting professor. Now he is co-leader of the Smart Antenna Research Team (SmART) at University of Duisburg-Essen.

Dr. Kaiser has published more than 80 papers in international journals and at conferences, and he is co-editor of three forthcoming books on Ultra-Wideband systems. Dr. Kaiser is founder of PLANET MIMO Ltd. and belongs to the editorial board of EURASIP Journal of Applied Signal Processing and to the advisory board of a European multi-antenna project. He is the founding Editor-in-Chief of the IEEE Signal Processing Society e-letter. His current research interest focuses on applied signal processing with emphasis on multi-antenna systems, especially its applicability to ultra-wideband systems.